Journal of Biological Physics **25:** 149–164, 1999.

Soliton-Like Regimes and Excitation Pulse Reflection (Echo) in Homogeneous Cardiac Purkinje Fibers: Results of Numerical Simulations

O.V. ASLANIDI and O.A. MORNEV
Institute of Theoretical and Experimental Biophysics of Russian Academy of Sciences, Pushchino, Moscow Region 142292, Russia
Author for correspondence: e-mail: mornev@venus.iteb.serpukhov.su

Accepted in final form 4 March 1999

Abstract. On the basis of numerical simulations of the partial McAllister-Noble-Tsien equations quantitatively describing the dynamics of electrical processes in conductive cardiac Purkinje fibers we reveal unusual – soliton-like – regimes of interaction of nonlinear excitation pulses governing the heart contraction rhythm: reflection of colliding pulses instead of their annihilation. The phenomenological mechanism of the reflection effects is that in a narrow (but finite) range of the system parameters the traveling pulse presents a doublet consisting of a high-amplitude leader followed by a low-amplitude subthreshold wave. Upon collisions of pulses the leaders are annihilated, but subthreshold waves summarize becoming superthreshold and initiating two novel echo-pulses traveling in opposite directions. The phenomenon revealed presents an analogy to the effect of reflection of colliding nerve pulses, predicted recently, and can be of use in getting insight into the mechanisms of heart rhythm disturbances.

Key words: Excitable media, Nonlinear waves, Heart, Reflection, Limit cycle bifurcation.

Introduction

Nonlinear wave processes lying at the basis of information transmission and control in biological systems attract broad interest of investigators. One of the organs whose normal functioning is essentially connected with processes of this kind is the heart.

Rhythmic contractions of muscular walls of the heart chambers (atria and ventricles) are initiated by nonlinear excitation waves – pulses of electrical recharge of heart cell membranes [1]. These waves (in many respects analogous to nerve pulses [2] and belonging to the class of autowaves [3]) are periodically emitted by the sino-atrial node – a local claster of self-generating cells in the right atrium – and from here propagating through the heart muscular tissue according to the following circuit (see detail in any textbook on general physiology):

sino-atrial node → atria → His' bundle fibers → Purkinje fibers

→ ventricle muscles. (1)

Fibers of the His' bundle and Purkinje fibers named here are specialized cable-like conductive structures, through which excitation pulses travel from atria to ventricles. Directed propagation of pulses along the pathway presented at the circuit (1) leads to correct alternations of the heart chambers contractions (first atria muscles contract, then ventricle muscles); respectively, any disturbances of this propagation disorder the consistent regime of contractions and lead to pathologies.

The well-known property of excitation pulses defining specificity of the heart performance (as well as performance of the nervous system) is that these pulses decay (are not reflected, but annihilated) upon collisions to each other and impermeable bounds of the excitable medium. Let's briefly remind of the mechanism of this phenomenon. The front of a traveling excitation pulse electrically recharging the membrane of cardiac cells is always followed by a refractory zone where reverse recharge and recovery of the membrane subsystems to the initial resting state occurs [1, 2]. In the refractory zone cell membranes are temporarily unexcitable, and this prevents passage through of two counter-propagating pulses, as well as emergence of reflected echo-waves.

The annihilation of colliding pulses plays a fundamental role in living organisms. For the heart, this effect is one of the facts providing stability of the directed propagation of electric excitation pulses along the pathway (1). If the pulses at any stretch of the pathway were not annihilated but reflected, then the directed flow of electric signals on this stretch would loose the stability: collision of any pulse of the flow with a single sporadic oncoming pulse would lead to a cascade of re-reflections disordering the flow.

Indeed, development of certain cardiac arrhythmias is associated namely with pulse reflection, and respective phenomena are intensively investigated. However, until recently all attempts were concerned with the mechanisms of reflection of traveling pulses at interactions with geometrical and/or functional heterogeneities of the excitable medium: a bit of experimental [4–5] as well as theoretical [6–8] work was done in this direction. As for the effects of reflection of excitation pulses after their collisions to each other and impermeable obstacles, the opinion that such effects are not feasible has until recently been challenged by no-one – in view of the quantitative argumentation based on the existence of the refractory zones. Moreover, the property of autowaves to decay at collisions is so universal (namely in this way behave combustion waves, concentration waves in chemical active media, etc.), that it has been long considered as a characteristic feature distinguishing this type of waves from solitons – nonlinear waves propagating in conservative media with dispersion (as is known, solitons escape interactions undestroyed) [9].

Recent results of numerical simulations refute the indicated opinion. In several works [10–16] performed with simplified mathematical models of homogeneous

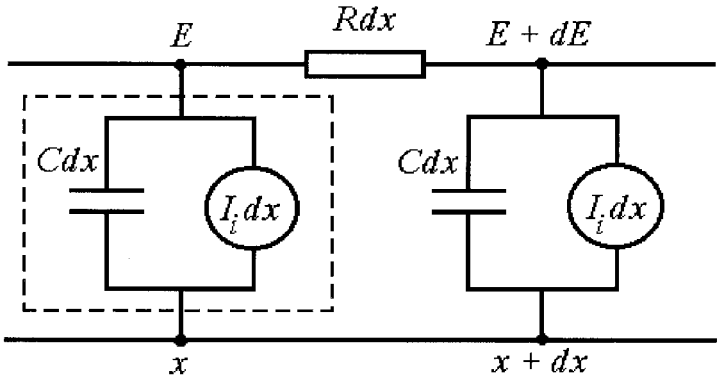

Figure 1. Equivalent electric circuit of a Purkinje fiber. Conductive outer medium is presented by a bus with zero resistance. The dotted frame embraces the local excitable unit described by the local kinetics equations (5).

excitable media unusual *soliton-like regimes* of propagating excitation pulse interaction were revealed: upon collisions to each other and impermeable medium bounds the pulses were not annihilated, but reflected! With that counter-samples refuting the opinion on impossibility of reflection of colliding autowaves were obtained. Afterwards stable soliton-like regimes were revealed in an adequate quantitative model of nerve fiber described by the well-known Hodgkin-Huxley equations [17, 18] that enabled pre-evaluation of conditions for observation of the reflection effect in direct physiological experiments [18]. These results immediately raise question on the possibility of existence of similar phenomena in cardiac tissue. According to stated above, the answer to this question presents apparent interest.

In the present work we announce results concerning investigation of the soliton-like regimes in the qualitative mathematical model of a Purkinje fiber presenting a stretch of the pathway (1).

A brief description of the model is given in Section 1; results of numerical experiments performed with this model are presented in Sections 2 and 3. In Section 4 phenomenological mechanisms of echo-pulse generation are considered. In conclusion we discuss the obtained results and outline the direction of further investigations.

1. The McAllister-Noble-Tsien Model of a Purkinje Fiber

In numerical simulations we used nonlinear reaction-diffusion equations whose reaction terms are taken from the known ordinary McAllister-Noble-Tsien equations [19] qualitatively describing the dynamics of ionic currents at the Purkinje fiber membrane. The resulting equations are as follows

$$\frac{\partial E}{\partial t} = D\frac{\partial^2 E}{\partial x^2} - \frac{1}{C}I_i; \tag{2a}$$

$$I_i = I_{\mathrm{Na}}(E, h, m; E_{\mathrm{Na}}) + I_{\mathrm{si}}(E, d, f) + I_{\mathrm{K}_1}(E) + I_{\mathrm{K}_2}(E, s)$$

$$+I_{X_1}(E, x_1) + I_{X_2}(E, x_2) + I_{\mathrm{Cl}}(E, q, r) + I_{\mathrm{Na,b}}(E; E_{\mathrm{Na}}) + I_{\mathrm{Cl,b}}(E); \quad (2b)$$

$$\frac{\partial z}{\partial t} = \alpha_z(E) \cdot (1 - z) - \beta_z(E) \cdot z, \quad z \in \{m, h, d, f, s, x_1, x_2, q, r\}; \quad (2c)$$

here the cable equation (2a) [20] describes the balance of currents and potentials in the electric equivalent circuit of a Purkinje fiber (see Figure 1); $E = E(x, t)$ [mV] is the intracellular electric potential of a Purkinje fiber (the extracellular potential is calibrated by zero); x [cm] is the distance along the fiber counted off its left end; t [ms] is time; $C = 10\ \mu\mathrm{F\ cm^{-2}}$ [19] is the capacitance of the Purkinje fiber membrane per unit membrane area; $D \equiv a/2RC = 0.01\ \mathrm{cm^2\ s^{-1}}$ is the diffusivity (here R is the specific internal resistance of a fiber, a is the fiber radius; this value of D was adopted from the condition of coincidence of the propagating pulse velocity obtained numerically with the experimental value of about 1 m $\mathrm{s^{-1}}$ [21]); I_i is the density of the total membrane ionic current per unit membrane area; I_{Na}, I_{si}, I_{K_1}, I_{K_2}, I_{X_1}, I_{X_2}, I_{Cl}, $I_{\mathrm{Na,b}}$, $I_{\mathrm{Cl,b}}$ in (2b) are densities of the currents which are carried by various ions and are given functions of their arguments (physiological sense of these currents and their dependence on arguments are indicated in [19]); E_{Na} is the sodium equilibrium potential appearing in expressions for the currents I_{Na} and $I_{\mathrm{Na,b}}$ (in our numerical experiments E_{Na} was the governing parameter, see Section 2); m, $h, d, f, s, x_1, x_2, q, r$ are kinetic variables and functions describing the dynamics of activation and inactivation of respective currents and obeying the kinetic equations (2c); $\alpha_z(E)$ and $\beta_z(E)$ are phenomenological functions (the analytical expressions for $\alpha_z(E)$ and $\beta_z(E)$ are given in [19]).

The cable equation (2a) with the McAllister-Noble-Tsien equations (2b,c) form a system of model reaction-diffusion equations of 10th order describing a Purkinje fiber. Usually the case of a fiber with electrically isolated boundaries located at the points $x = 0, L$ is considered; in this case the system (2) is supplemented with the boundary conditions

$$\left.\frac{\partial E}{\partial x}\right|_{x=0} = 0, \qquad \left.\frac{\partial E}{\partial x}\right|_{x=L} = 0, \quad (3a,b)$$

describing impermeability of the boundary sections of the fiber for the total electric current

$$I(x, t) = -\frac{\sigma}{R}\frac{\partial E(x, t)}{\partial x} = -\frac{\pi a^2}{R}\frac{\partial E(x, t)}{\partial x}, \quad (4)$$

flowing in the longitudinal direction ($\sigma = \pi a^2$ is the area of the fiber section).

With the system of equations (2) the system of *local kinetics equations* is closely connected, which is obtained from (2) by neglecting the diffusion term in (2a) and having the form

$$C\frac{dE}{dt} = -I_i(E, z; E_{\mathrm{Na}}); \quad \frac{dz}{dt} = \alpha_z(E)\cdot(1-z) - \beta_z(E)\cdot z; \tag{5}$$

here $I_i(E, z; E_{\mathrm{Na}})$ is the short denomination of the left-hand part of (2b).

The system (5) describes the properties of a *local excitable unit* (put in a dotted frame in Figure 1) that is a small fiber segment of dx length, electrically isolated ($R \to \infty$) from other sites of the fiber. Also note, that solutions $E = E(t), z = z(t)$ to the ordinary local kinetics equations (5) are also spatially uniform solutions to the partial reaction diffusion equations (2) at boundary conditions (3).

Under our consideration both systems (2) and (5) are dependent on the free parameter E_{Na}.

2. Search of the Soliton-Like Regimes. I. Detection of the Global Limit-Cycle Bifurcation in the Ordinary Equations of Local Kinetics

As it was shown in the papers [17, 18] cited above, reflection of colliding nerve pulses in the partial Hodgkin-Huxley equations is observed when the corresponding ordinary system of local kinetics is close to the global limit-cycle bifurcation*. The same holds for a simplified mathematical model of excitable medium described by the well-known FitzHugh-Nagumo equations [15].

These facts inspired us to advance a hypothesis that closeness of the ordinary local kinetics equations to the global limit bifurcation is the necessary condition for emergence of the soliton-like solutions to the respective partial reaction-diffusion equations [15, 17, 18].

Search of the soliton-like regimes in the McAllister-Noble-Tsien equations (2) was based on the stated hypothesis. At the first step we searched numerically the limit-cycle bifurcation in the ordinary local kinetics equations (5) under variations of the sodium equilibrium potential E_{Na}. The choice of E_{Na} as the governing parameter was inspired by the following reasons.

- At physiologically normal conditions (which correspond to the value $E_{\mathrm{Na}} =$ 40 mV) an isolated Purkinje fiber performs as self-oscillating system periodically generating excitation pulses [1, 2, 19].
- Decreasing the value of E_{Na} sufficiently in comparison with the norm (experimentally it is achieved by decreasing the sodium ion concentration in outer solution bathing the fiber) one can transfer the fiber from self-oscillations into the excitable regime [1, 2].

* Far from the bifurcation the system has one of the following attractors: either a stable steady state, or a stable limit cycle. In these cases the local excitable unit of a nerve fiber presents either a monostable excitable system (capable to generate a single nerve pulse in response to supercritical external perturbations), or a self-oscillating system. Close to the bifurcation at supercritical values of the governing parameter both attractors coexist and, depending on initial conditions, the system either passes to the steady state (resting regime) or generates pulse in self-oscillating regime.

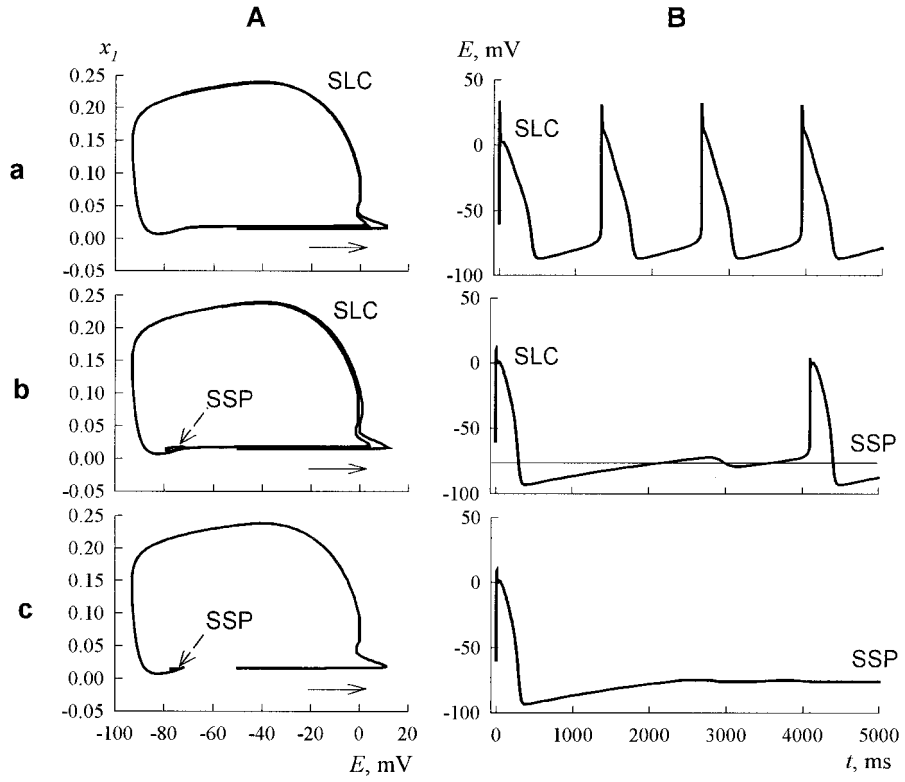

Figure 2. Qualitative properties of the system of local kinetics equations (5) at different values of the parameter E_{Na}. Column A shows projections of the stable limit cycle (SLC) and the stable steady point (SSP) of system (3) on the plane of variables (E, x_1), while in column B the corresponding dependencies of the potential E on time t are presented. Line a: $E_{\mathrm{Na}} = 40$ mV; line b: $E_{\mathrm{Na}} = 12.93$ mV; line c: $E_{\mathrm{Na}} = 12$ mV.

- The system of ordinary equations (5) at the normal value $E_{\mathrm{Na}} = 40$ mV is also a self-oscillating one, and respective solutions are in good quantitative agreement with experimental data [19].

Thus, relying on the facts listed above one can expect that decrease of E_{Na} will lead to transition of the system (5) from the self-oscillating regime to the excitable one; besides, it is hoped that the transition will follow the pattern seen at the global limit-cycle bifurcation (see the first footnote).

Such transition was actually revealed in our numerical experiments, and it evolved according to the scenario of the pointed bifurcation.

In experiments the range 12 mV $\leq E_{\mathrm{Na}} \leq$ 40 mV was investigated. The presence of self-oscillations in the system (5) at fixed E_{Na} was tested numerically; besides, the coordinates $E_0(E_{\mathrm{Na}})$, $z_0(E_{\mathrm{Na}})$ of steady ($\equiv$ resting) points of the

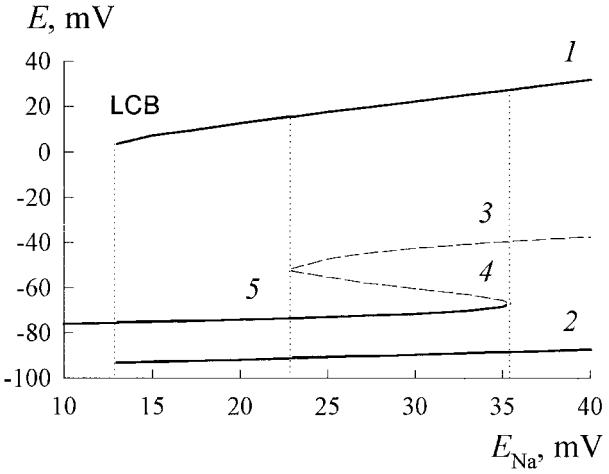

Figure 3. Bifurcation diagram of the system of local kinetics equations (5). Curves *1* and *2* present dependences of the maximal and the minimal values of the variable E on the stable limit cycle on the value E_{Na}, curves *3–5* present dependencies of the coordinates E_0 of steady points of system (5) on E_{Na} (curves *3*, *4* correspond to unstable steady points, curve *5* corresponds to the stable one). LCB indicates the global limit-cycle bifurcation.

system (5) were found and stability of the points was determined⋆. The results of computations are presented in Figures 2 and 3.

Figure 2 illustrates the behavior of the ordinary system (5) at three different values of E_{Na}. At the normal value $E_{\mathrm{Na}} = 40$ mV self-oscillations are observed confirming the data of [19]; in this case a stable limit cycle coexists with an unstable steady point (see Figure 2, line a). In accordance with expectations the decrease of E_{Na} transfers the system (5) to the excitable regime. Prior to the transition the stable limit cycle coexists with a stable steady point (see Figure 2, line b); this is a typical pattern preceding the global limit-cycle bifurcation. After the transition the limit cycle disappears and only one attractor, the stable resting point, remains in the system (5) (see Figure 2, line c). More detailed information on qualitative properties of the system (5) is presented on the bifurcation diagram (see Figure 3).

Because the limit cycle and resting points of the ordinary system (5) determine spatially uniform time-periodic and steady solutions to the partial reaction-diffusion equations (2) at boundary conditions (3), the diagram in Figure 3 contains

⋆ At given E_{Na} the coordinates $E_0(E_{\mathrm{Na}})$, $z_0(E_{\mathrm{Na}})$ of each steady point were determined by solving the equations $I_i(E_0, z_0; E_{\mathrm{Na}}) = 0$, $z_0 = \tilde{z}(E_0) \equiv \alpha(E_0)[\alpha(E_0) + \beta(E_0)]^{-1}$ obtained from the system (5) at $\dot{E} = \dot{z} = 0$; doing so the coordinate $E_0(E_{\mathrm{Na}})$ was numerically found from the equation $I_i(E_0, \tilde{z}(E_0); E_{\mathrm{Na}}) = 0$, then the coordinate $z_0(E_{\mathrm{Na}})$ was evaluated (for each variable z) as $z_0(E_{\mathrm{Na}}) = \tilde{z}[E_0(E_{\mathrm{Na}})]$. Stability of steady points was investigated by numerical integration of the system (5) at initial values of E, z from a small vicinity of the point. In all cases the integration was performed by the Runge-Kutta method with time step $ht = 0.004$ ms ($ht = 0.001$ ms in control experiments).

also information on ranges of existence and stability of these solutions. Particularly, the figure shows that stable steady solution

$$E(x,t) \equiv E_0(E_{\mathrm{Na}}); \quad z(x,t) \equiv z_0(E_{\mathrm{Na}}) \tag{6}$$

to the reaction-diffusion equations (2), describing the resting state of a Purkinje fiber with electrically isolated boundaries exists only at $E_{\mathrm{Na}} \leq 35.38$ mV, because curve 5 in Figure 3 presenting the dependence of the resting potential E_0 of the fiber on E_{Na} exists only when the inequality is satisfied. Hence, the problem of obtaining the traveling pulse solutions to the reaction-diffusion system (2) seems reasonable namely in this range. The solutions can be found by numerical integration of equations (2) at initial conditions

$$E(x,0) \equiv E_0(E_{\mathrm{Na}}), \;\; z(x,0) \equiv z_0(E_{\mathrm{Na}}) \quad (E_{\mathrm{Na}} \leq 35.38 \text{ mV}) \tag{7}$$

following from (6) and at the boundary conditions describing initiation of excitation pulses at the ends of the fiber (see below, next section).

It is important that the range of E_{Na} values corresponding to the existence of the stable steady state of the Purkinje fiber contains the point of the global limit-cycle bifurcation: the latter is implemented in the ordinary system (5) at $E_{\mathrm{Na}} = 12.93$ mV (see Figure 3). According to the hypothesis stated at the beginning of this section, one can expect that the colliding pulse reflection phenomena, if they do exist in the partial system (2), will emerge right close to the bifurcation value of E_{Na}. The expected soliton-like regimes were actually revealed in numerical experiments described in the next section.

3. Search of the Soliton-Like Regimes. II. Numerical Experiments with the Partial McAllister-Noble-Tsien Equations near the Bifurcation Value of E_{Na}

The system of reaction-diffusive equations (2) was integrated according to the three-point explicit scheme at the segment $0 \leq x \leq L$ simulating a Purkinje fiber. The steps of numerical integration in time and in space were $hx = 0.3$ cm and $ht = 0.004$ ms ($hx = 0.1$ cm and $ht = 0.001$ ms in control simulations). The initial conditions were given according to (7). In the simulations the effects following collision of a traveling pulse with impermeable obstacle and collision of two pulses were studied.

3.1. COLLISION OF A PULSE WITH AN IMPERMEABLE OBSTACLE

The obstacle was the right end of the fiber with the boundary condition of impermeability (3b) supported. The pulse was initiated at the left end of the fiber by setting the boundary condition

$$\left.\frac{\partial E}{\partial x}\right|_{x=0} = \begin{cases} p \equiv -100 \text{ mV cm}^{-1} & \text{at } t \in [0,T],\ T = 10 \text{ ms}, \\ 0 & \text{at } t > T, \end{cases} \tag{8}$$

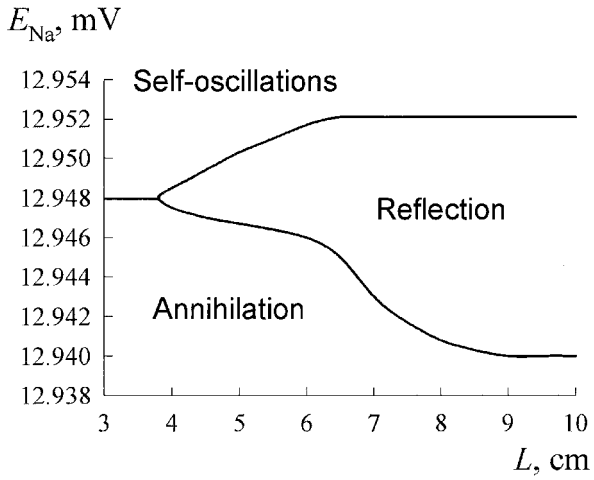

Figure 4. Diagram of regimes in the reaction-diffusion system (2) on the plane of parameters (L, E_{Na}). The minimal value $L = 3$ cm of the chosen range is greater then specific length of the traveling front (about 1 cm) and, therefore, it is correct to speak about wave propagation in all the range presented.

and then propagated rightward and collided to the right fiber boundary⋆. Phenomena accompanying the collision were observed in consequent series of experiments. In each series the fiber length L was given (is was altered from one series to another), and the regimes of pulse interaction were studied for the given L at different values of E_{Na} from the interval indicated in (7). As the result we obtained the subdivision of the plane of parameter (L, E_{Na}) at regions corresponding to the following three regimes (Figure 4).

Annihilation regime. This regime is usual: a pulse colliding to the impermeable right boundary decay (is annihilated) (see Figure 5) and the fiber passes with time to the resting state (6).

Soliton-like regime. In this regime a pulse colliding to the impermeable right boundary of the fiber is reflected (*echo*, see Figure 6), travels backward and collides with the left boundary, where by that time the impermeability condition coinciding with (3a) is supported (see footnote 3). A new act of reflection occurs and the reflected echo-pulse travels rightward again. The reflection cycle reoccurs again and again without any changes. This experimental fact shows that the soliton-like regimes are described by stable spatially uniform time-periodic solutions to the partial McAllister-Noble-Tsien equations (2) (with boundary conditions (3)). As

⋆ Condition (8) means that at the moment $t = 0$ the fiber is connected to the external source of constant electric current. The current is delivered to the left section of the fiber during a finite time interval of T duration, initiating a pulse; then the source is switched off and the impermeability condition (3a) is settled at the point $x = 0$. The current intensity is connected to the value p in (8) by (4). The values of p and T in (8) were chosen so that the impermeability condition at the fiber left boundary settle before the traveling pulse collided with the right boundary.

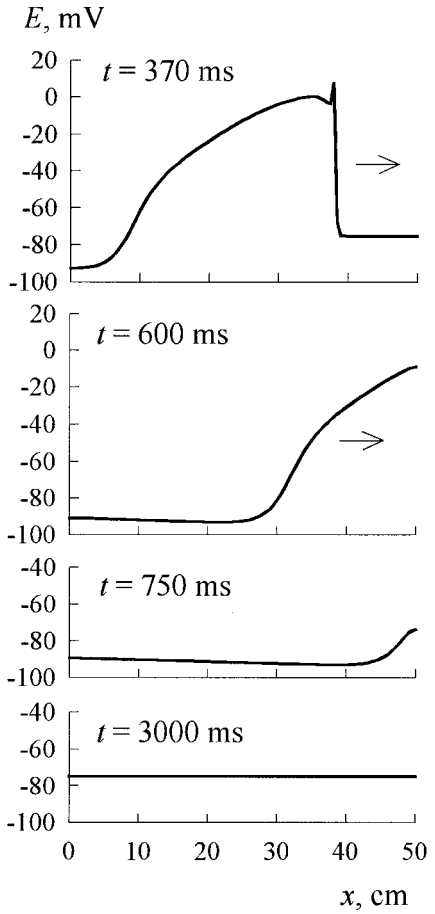

Figure 5. Annihilation regime in the reaction-diffusion system (2) ($L = 50$ cm, $E_{\mathrm{Na}} = 15$ mV). Here and in Figures 6 and 7 profiles of the potential E are presented at indicated time moments t. An excitation pulse traveling rightward decays (is annihilated) upon collision to the right impermeable end of the fiber. To illustrate the spatial structure of traveling waves at this figure, as well as at following ones, parameter L was set at abnormally high value.

follows from comparison of the diagrams in Figures 3 and 4, the soliton-like regime is implemented in system (2) when the E_{Na} values are close to the critical value, corresponding to the global limit cycle bifurcation in the local kinetics equations (5).

Self-oscillation regime. In this regime a finite duration impulse of the the internal current, described by the boundary condition (8), switches the fiber into the self-oscillation regime: the left end of the fiber starts to emit pulses traveling rightward. Patterns of pulse propagation and interaction with the right boundary (reflection is not observed) is qualitatively analogous to that obtained in [17, 18]

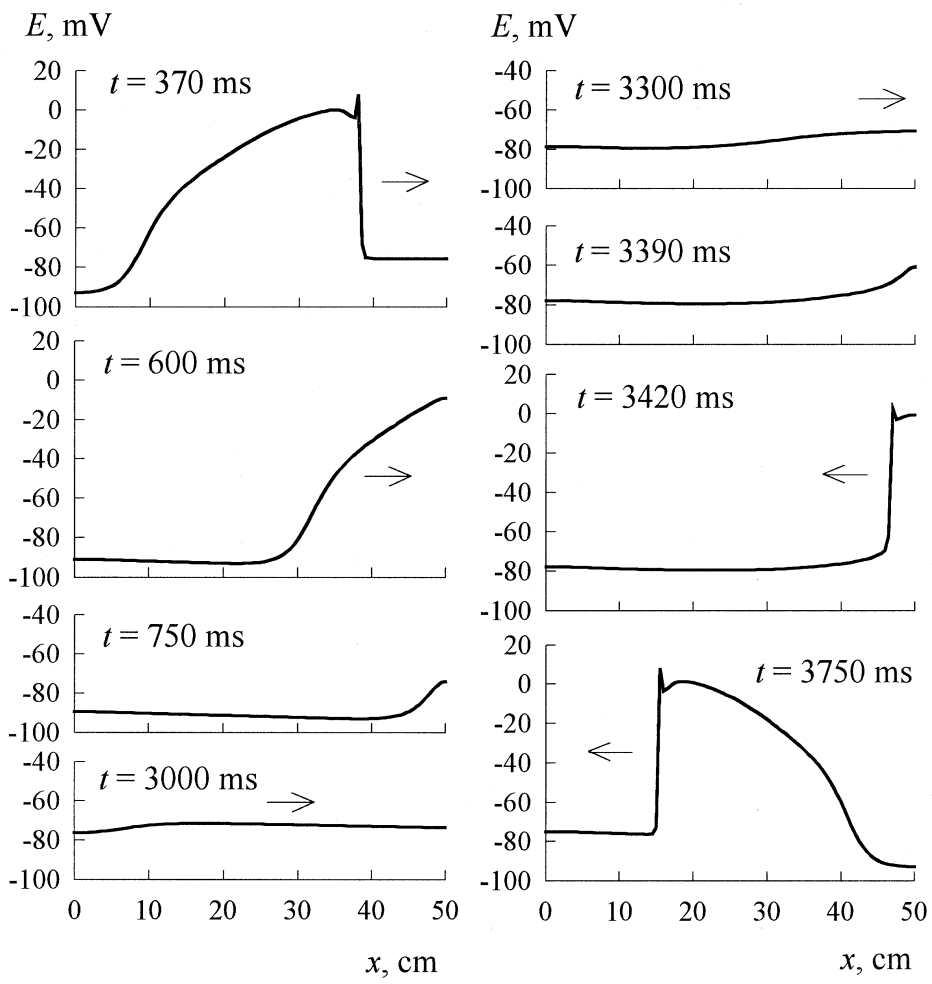

Figure 6. Soliton-like regime in the reaction-diffusion system (2) ($L = 50$ cm, $E_{Na} = 12.94$ mV). An excitation pulse traveling rightward does not decay after collision to the right impermeable end of the fiber, but is reflected.

at integration of the Hodgkin-Huxley equations describing squid axon, and is not presented here. This space-inhomogeneous regime of pulse generation is presumably a transitional one: it can be expected that oscillation in different points of the fiber will become synchronous with time, as it occurs in the case of the FitzHugh-Nagumo equations [15], and will correspond to the limit cycle of the local kinetics equations (5). Further investigations are necessary in this direction.

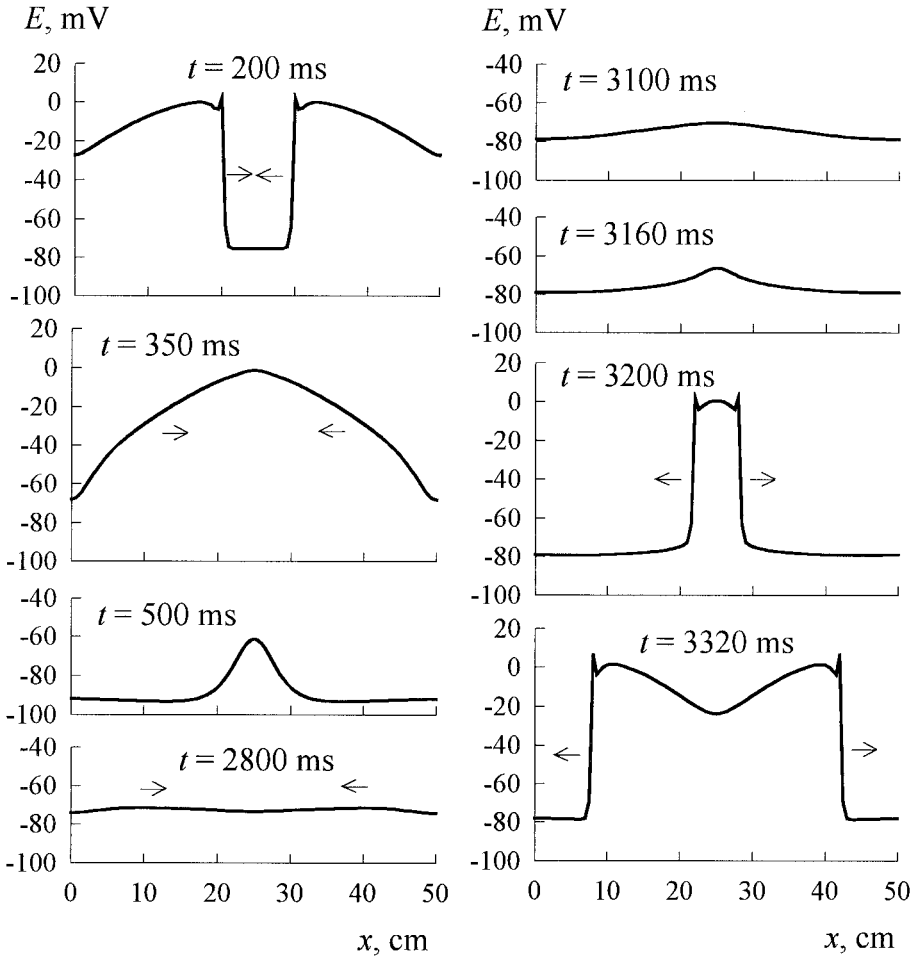

Figure 7. Soliton-like regime in the reaction-diffusion system (2) ($L = 50$ cm, $E_{\mathrm{Na}} = 12.94$ mV) at collision of pulses traveling from the fiber ends in oncoming directions. After collision the pulses are reflected back and travel in opposite directions.

3.2. COLLISION OF ONCOMING PULSES

In this case excitation pulses were initiated simultaneously at both ends of the fiber by setting the following boundary conditions

$$\left.\frac{\partial E}{\partial x}\right|_{x=0} = -\left.\frac{\partial E}{\partial x}\right|_{x=L} = \begin{cases} p \equiv -100 \text{ mV cm}^{-1} & \text{at } t \in [0, T], \ T = 10 \text{ ms}, \\ 0 & \text{at } t > T, \end{cases} \tag{9}$$

and traveled towards each other colliding at the point $x = L/2$. As well as in the previous case the effects accompanying the collision were studied at different L and E_{Na}. The corresponding diagram is not presented for it differs from that in Figure 4

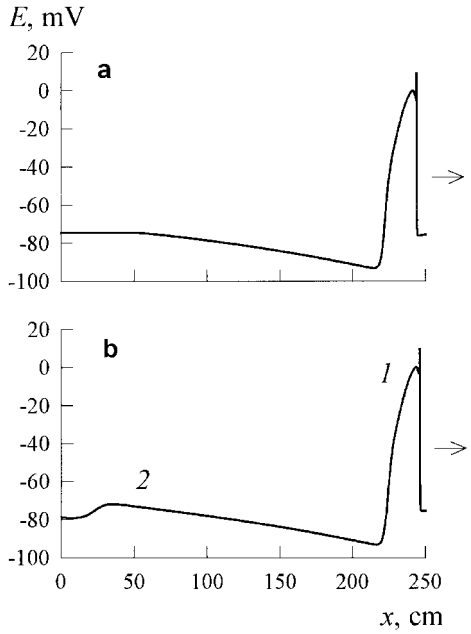

Figure 8. Spatial profiles of traveling excitation pulses obtained by numerical integration of the McAllister-Noble-Tsien equations under conditions of the annihilation (a) and the soliton-like (b) regimes (arrows indicate the direction of pulse propagation). a – $E_{\mathrm{Na}} = 15$ mV; b – $E_{\mathrm{Na}} = 12.94$ mV. It is clear that in the soliton-like regime a traveling excitation pulse presents the doublet consisting of high-amplitude leader *1* followed by low-amplitude wave *2*.

by the scale at the axis L only: according to the symmetry reasons the qualitative effects accompanying collision of oncoming pulses in a fiber with the length L has no difference from the effects upon collision of a single pulse with the impermeable bound of a fiber of $L/2$ length (at oncoming propagation of the pulses symmetric in respect to the point $x = L/2$, the equality $(\partial E/\partial x)|_{x=L/2} = 0$ is satisfied at this point at any time moment). At the values of L and E_{Na} corresponding to the soliton-like regime, colliding pulses are reflected (Figure 7), travel in opposite direction, are reflected from the impermeable bounds and travel towards each other again. Then all the effects are repeated.

4. Why Are They Reflected?

To answer this question, let us compare instant spatial profiles of excitation pulses traveling along the fiber under conditions of the usual annihilation regime (see Figure 8a), with those under conditions of the soliton-like one (see Figure 8b).

It can be seen from the figure that in the soliton-like regime the traveling excitation pulse is followed by a subthreshold depolarization wave, which is absent in the case of the annihilation regime; in other words, in the soliton-like regime the

traveling pulse presents a doublet consisting of a high-amplitude pulse-leader and a low-amplitude wave following the pulse (note, that a nerve pulse in the soliton-like regime is characterized by the same wave structure [18]). Namely the existence of these subthreshold waves causes reflection of the doublets after their collisions and annihilation of leading pulses. Qualitative reasonings confirming the aforesaid are as follows.

Let's first consider the case of reflection of such a doublet from the impermeable fiber boundary. The leading pulse traveling rightward first collides the right boundary (Figure 6, $t = 600$ ms) and is annihilated (Figure 6, $t = 750$ ms); with a short delay the subthreshold wave (Figure 6, $t = 3000$ ms) also reaches the boundary (Figure 6, $t = 3300$ ms), collides with it, becomes superthreshold (Figure 6, $t = 3390$ ms) and initiates a reflected excitation pulse traveling leftward (Figure 6, $t = 3420$ ms). The question is why the low-amplitude wave which is subthreshold at propagation along the fiber becomes superthreshold after collision with the impermeable obstacle? The explanation is as follows. To each propagating wave an axial gradient of electric potential is related; according to expression (2), the gradient induces internal axial electric currents flowing on the wave edges along the fiber. When the subthreshold wave approaches the boundary impermeable for the axial current, all the current flowing forward from the front of the wave starts now to flow through the fiber membrane. That leads to such an increase of the total membrane ionic current density that is enough to shift the membrane potential E near the boundary to the superthreshold value causing regeneration of the initial pulse. Hence, a low-amplitude wave colliding with an obstacle behaves as "generator" emitting an echo-pulse.

Reflection of two colliding doublets evolves according to the same scenario (see Figure 7) due to the symmetry reasons presented in the previous section.

The results of numerical simulations confirming the necessity of low-amplitude waves for reflection of colliding pulses will be published elsewhere.

5. Conclusion

The results obtained in the present work have several aspects.

We confirm that the soliton-like regimes in reaction-diffusion equations describing biological excitable media are not "exotic", but "standard" qualitative phenomena implemented at certain conditions. The universal phenomenological mechanism of echo-wave generation at pulse collisions to each other and impermeable obstacles is also revealed: it is connected to the existence of subthreshold waves following full-amplitude traveling pulses. Note, that such low-amplitude waves are often recorded in physiological experiments, the slow voltage alteration forming the wave being called *delayed afterdepolarization* [1, 22, 23]. In special literature this phenomenon was discussed in connection to its possible role in some cardiac pathological regimes – so-called triggered activity [1]: the latter are manifested as a superthreshold stimulation applied to the cardiac ex-

citable tissue leading at certain conditions to emergence of premature electrical pulsation [22, 23]. However, experimental cardiology has not yet clarified either the mechanisms of triggered arrhythmias, or the reasons for the appearance of delayed afterdepolarization waves; presumably, the role of these waves as potential echo-pulse generators has not been realized yet. The numerical simulations performed clarify the situation to some extent: according to the computation results, traveling doublets "high-amplitude leader + low-amplitude wave of delayed afterdepolarization" should be observed in the region of the governing parameter values, separating excitable and self-oscillation regimes, where the system of local kinetics equations is close to the global limit-cycle bifurcation. In the neighborhood of this bifurcation the mentioned system has two attractors – a steady point and a limit cycle responsible for generation of excitation pulses; herewith transition of the system from one attractor to another can be realized by a superthreshold perturbation. Such local dynamics remarkably resembles the dynamics of triggered activity, and both phenomena – the waves of delayed afterdepolarization and the triggered activity – could present different dynamic manifestations of similar conditions arising in excitable media. Of course, it is of first importance to understand the manner in which the limit-cycle bifurcation of ordinary local kinetic equations predetermines the doublet structure and reflection of running excitation pulses.

All the results of this work were obtained in frameworks of the McAllister-Noble-Tsien model describing electrical phenomena in cardiac Purkinje fibers. Although these results allow planning physiological experiments to observe the predicted effects, it should be mentioned that the model used is not as adequate as more recent DiFrancesco-Noble equations [24] proposed for the same object; therefore, quantitative conditions for implementation of the soliton-like regimes in Purkinje fibers have to be elaborated using the latter equations (preliminary numerical simulations carried out by the authors confirmed the existence of soliton-like regimes in the DiFrancesco-Noble equations). Finally, note that Purkinje fibers are only one of the elements on the pathway of excitation pulse propagation from the sinoatrial node to the ventricles, presented by circuit (1). It would be interesting to investigate the possibility of existence of soliton-like regimes in other elements of the pathway evolving respective equations – up to date they have been described elsewhere. Thus, the cardiac structures where echo-like arrhythmias are possible would be revealed. The aforesaid contains the program of further investigations.

This work was supported by the grant RFBR No. 990100956.

References

1. Zipes, D.P., Jalife, J. (eds.): *Cardiac electrophysiology*, Philadelphia, Sanders Co., 1990.
2. Khodorov, B.I.: *General physiology of excitable membranes*, Moscow, Nauka, 1975 (in Russian).
3. Krinsky, V.I. (ed.): *Self-organization. Autowaves and structures far from equilibrium*, Berlin, Springer, 1984.

4. Howe, J.F., Calvin, V.H. and Loeser, J.D.: Impulses reflected from dorsal root ganglia and from focal nerve injuries, *Brain Res.* **116** (1976), 139–144.
5. Antzelevich, C., Jalife, J. and Moe, G.K.: Characteristics of reflection as a mechanism of reentrant arrythmias and its relationship to parasystole, *Circulation* **61** (1980), 182–191.
6. Krinsky, V.I. and Kholopov, A.V.: Echo phenomenon in excitable tissue, *Biofizika* **12** (1967), 524–528 (in Russian).
7. Cabo, C. and Barr, R.C.: Reflection after delayed excitation in a computer model of a single fiber, *Circ. Res.* **71** (1992), 260–270.
8. Ermentrout, B. and Rinzel, J.: Reflected waves in an inhomogeneous excitable medium, *SIAM J. Appl. Math.* **56** (1996), 1107–1128.
9. Scott, A.C., Chu, F.Y.E. and McLaughlin, D.W.: Solitons – a new concept in applied sciences, *Proc. IEEE* **61** (1973), 1443–1483.
10. Tuckwell, H.C.: Solitons in a reaction-diffusion system, *Science* **205** (1979), 493–495.
11. Rotermund, H., Jakubith, S., Oertzen, H. and Ertl, G.: Solitons in a surface reaction, *Phys. Rev. Lett.* **66** (1991), 3083–3086.
12. Kobayashi, R., Ohta, T. and Hayase, Y.: Self-organized pulse-generator in reaction-diffusion system, *Phys. Rev. E* **50** (1994), R3291–R3294.
13. Petrov, V., Scott, S.K. and Showalter, K.: Excitability, wave reflection and wave splitting in a cubic autocatalysis reaction-diffusion system, *Phil. Trans. R. Soc. A* **347** (1994), 631–642.
14. Kosek, J. and Marek, M.: Wave reflection in reaction-diffusion equations, *Phys. Rev. Lett.* **74** (1995), 2134–2137.
15. Mornev, O.A., Aslanidi, O.V., Aliev, R.R. and Chailakhyan, L.M.: Soliton regimes in the FitzHugh-Nagumo model: Reflection of colliding pulses of excitation, *Doklady Biophys.* **346–348** (1996), 21–23.
16. Mornev, O.A., Aslanidi, O.V. and Chailakhyan, L.M.: Solitonic mode in the FitzHugh-Nagumo equations: Dynamics of a rotating spiral wave, *Doklady Biophys.* **352–354** (1997), 29–32.
17. Aslanidi, O.V. and Mornev, O.A.: Reflection of running excitation impulses, *Biophysics* **41** (1996), 967–973.
18. Aslanidi, O.V. and Mornev, O.A.: Can colliding nerve pulses be reflected?, *JETP Lett.* **65** (1997), 579–585.
19. McAllister, R.E., Noble, D. and Tsien, R.W.: Reconstruction of the electrical activity of cardiac Purkinje fibres, *J. Physiol. (Lond.)* **251** (1975), 1–59.
20. Scott, A.C.: Neurophysics of a nerve fiber, *Rev. Mod. Phys.* **47** (1975), 487–555.
21. Walton, M.K. and Fozzard, H.A.: Experimental study of the conducted action potential in cardiac Purkinje strands, *Biophys. J.* **44** (1983), 1–8.
22. Schechter, E., Freenam, C.C. and Lazzara, R.: Afterdepolarizations as a mechanism for the long QT syndrome, *J. Am. Coll. Cardiol.* **3** (1984), 1556–1561.
23. Wit, A.L. and Rosen, M.R.: Afterpolarizations and triggered activity, in H.A. Fozzard et al. (eds.), *The Heart and the Cardiovascular System*, Raven Press, 1986, pp. 1449–1490.
24. DiFrancesco, D. and Noble, D.: A model of cardiac electrical activity incorporating ionic pumps and concentration changes, *Phil. Trans. R. Soc.* **307** (1985), 353–398.